

Off-diagonal cumulants of net-charge, net-proton and net-kaon multiplicity distributions in Au+Au collisions at $\sqrt{s_{NN}} = 7.7\text{-}200$ GeV from STAR

Arghya Chatterjee* (for the STAR collaboration)

Variable Energy Cyclotron Centre, HBNI, Kolkata-700064, India

E-mail: arghya@vecc.gov.in

Fluctuations of conserved quantities such as net-baryon, net-charge, and net-strangeness numbers have generated considerable interest in the study of the thermodynamic properties of the hot and dense QCD matter. Theoretical calculations suggest that the off-diagonal cumulants of conserved charges along with the diagonal cumulants can help better constrain the freeze-out parameters and, therefore, help to map the QCD phase diagram. In this proceeding, we briefly outline the recent STAR measurements [1] on the second-order off-diagonal cumulants of net-charge, net-proton, and net-kaon multiplicity distributions in Au+Au collisions from the RHIC BES-I program in the energy range of $\sqrt{s_{NN}} = 7.7\text{-}200$ GeV. The measured cumulant ratios are compared to the predictions from both thermal (HRG) and non-thermal (UrQMD) models.

Corfu Summer Institute 2018 "School and Workshops on Elementary Particle Physics and Gravity" (CORFU2018)

31 August - 28 September, 2018

Corfu, Greece

*Speaker.

1. Introduction

The major goal of relativistic heavy-ion collision experiment is to study the formation of a new form matter, called the Quark-Gluon Plasma (QGP). Over the last two decades, a number of possible evidences for the QGP phase has been established experimentally. Currently a large community of physicists are exploring the QCD phase structure and trying to find a possible signature of the QCD critical point. One of the most community used method to explore phase diagram is to study the event-by-event fluctuations of conserved charges, such as net electric charge (Q), net baryon number (B) and net strangeness number (S) in the heavy-ion collisions over a wide range of energy [2, 3]. It is proposed that the higher-order cumulants of the net-multiplicity distributions are related to the higher order thermodynamic susceptibilities of corresponding conserved charges in QCD and expected to diverge near the critical point [2, 4]. Over the past few years, STAR and PHENIX experiments at RHIC published results on the diagonal cumulants (c_α^n) of net-electric charge [5, 6], net-proton (p , an experimental proxy for net-baryon) [7, 8] and net-kaon (k , an experimental proxy for net-strangeness) [9] multiplicity distributions. Similarly, off-diagonal cumulants ($c_{\alpha,\beta}^{m,n}$) of Q, p and k are related to the mixed susceptibilities that carry the correlation between different conserved charges [1]. Lattice QCD and hadron resonance gas model (HRG) calculations show that normalized baryon-strange correlations, that can be expressed as off-diagonal to diagonal cumulant ($C_{BS} = c_{B,S}^{1,1}/c_S^2$), are expected to be sensitive to the onset of deconfinement [10]. Another importance of studying off-diagonal cumulants is that it can also be used to constrain the freeze-out parameters in the QCD phase diagram. Different theoretical calculations demonstrate that the 2^{nd} -order off-diagonal cumulants show a significant sensitivity to the difference between HRG and lattice calculations [11, 12].

In this report, we present the measurements of 2^{nd} -order diagonal and off-diagonal cumulants of net charge, net proton and net kaon multiplicity distributions in Au+Au collisions ranging in center of mass energy from $\sqrt{s_{NN}} = 7.7$ to 200 GeV, with data taken during the first phase of RHIC Beam Energy Scan (BES-I).

2. Observables

The susceptibilities of the conserved charges of a system in thermal and chemical equilibrium (for a grand-canonical ensemble) can be computed from the partial derivatives of the dimensionless pressure with respect to the chemical potentials:

$$\chi_{B,Q,S}^{m,n,l} = \frac{\partial^{m+n+l}(P/T^4)}{\partial^m(\mu_B/T)\partial^n(\mu_Q/T)\partial^l(\mu_S/T)}, \quad (2.1)$$

where V and T are the system pressure and temperature, respectively, and $m, n, l = 1, 2, 3, \dots, n$ are the order of derivative. μ_Q , μ_B and μ_S are the electric charge, baryon and strangeness chemical potentials, respectively. The P is obtained from the logarithm of the QCD partition function:

$$P = \frac{T}{V} \ln[Z(V, T, \mu_B, \mu_Q, \mu_S)]. \quad (2.2)$$

These susceptibilities can be related to the cumulants (c) of the event-by-event distribution of the associated conserved charges by [3, 13, 14]:

$$\chi_{B,Q,S}^{m,n,l} = \frac{1}{VT^3} c_{B,Q,S}^{m,n,l}. \quad (2.3)$$

Due to the limitation in detecting all baryons and strange hadrons experimentally, net proton (p) and net kaon (k) are considered as proxies for the net baryon and net strangeness, respectively. In this report, we present the measurement of second-order ($m + n + l = 2$) diagonal and off-diagonal cumulants of net charge, net proton and net kaon multiplicity distributions, can be expressed as:

$$c_\alpha^2 = \sigma_\alpha^2 = \langle (\delta N_\alpha)^2 \rangle \quad \text{and} \quad c_{\alpha,\beta}^{1,1} = \sigma_{\alpha,\beta}^{1,1} = \langle (\delta N_\alpha)(\delta N_\beta) \rangle, \quad (2.4)$$

where α and β can be Q , p or k , and $\delta N_\alpha = (N_{\alpha^+} - N_{\alpha^-}) - \langle (N_{\alpha^+} - N_{\alpha^-}) \rangle$. Finally, we construct the off-diagonal to diagonal cumulant ratios ($C_{p,k} = c_{p,k}^{1,1}/c_k^2$, $C_{Q,p} = c_{Q,p}^{1,1}/c_p^2$ and $C_{Q,k} = c_{Q,k}^{1,1}/c_k^2$) motivated by Ref. [10], which also cancel the volume dependence.

3. Experimental details

Second-order cumulants of net charge, net proton and net kaon multiplicity distributions for Au+Au collisions at $\sqrt{s_{\text{NN}}} = 7.7, 11.5, 14.5, 19.6, 27, 39, 62.4$ and 200 GeV have been studied in the STAR experiment. The minimum-bias (MB) events are analyzed with the requirement that the position of the primary vertex along z -direction (V_z) was reconstructed within ± 30 cm of the center of the STAR detector and within 2 cm on the transverse plane of the beam axis. The number of events analyzed at each energy after applying all event selections criteria is listed in Table 1.

$\sqrt{s_{\text{NN}}}$ (GeV)	Year	Events ($\times 10^6$)
7.7	2010	1.5
11.5	2010	2.5
14.5	2014	12.7
19.6	2011	15.6
27	2011	25.2
39	2010	62.3
62.4	2010	31
200	2011	74

Table 1: Summary of the number of events analyzed.

All charged tracks used in this analysis are required to be within the pseudorapidity range $|\eta| < 0.5$, and the transverse momentum range $0.4 < p_T < 1.6$ GeV/ c . To reduce the contamination from the secondary charged particles, only primary tracks are selected within a distance of closest approach (DCA) to the primary vertex of less than 1 cm. The main detectors used in this analysis are the Time Projection Chamber (TPC) and the Time of Flight (TOF). The particle identification (PID) is done with a common acceptance: $0.4 < p_T < 1.6$ GeV/ c and $|\eta| < 0.5$. Within

this range, the purities of K^\pm and $p(\bar{p})$ identification is estimated to be 98-99%. The collision centrality for this analysis is defined using uncorrected charged particle multiplicity measured within a pseudorapidity range of $0.5 < |\eta| < 1.0$ in the TPC detector. This way we exclude the particles from the analysis region to determine the centrality in order to suppress autocorrelation effects [15]. We present the results for nine centrality bins, 0-5% (most central), 10-20%, ... , 70-80% (most peripheral) as a function of average number of participating nucleons ($\langle N_{part} \rangle$) estimated using a Monte Carlo Glauber model [16]. The cumulants and their ratios were calculated as a function of the reference multiplicity and then averaged over the centrality bins to suppress the volume fluctuations over wide centrality bins [17, 18]. We use embedding Monte Carlo simulation techniques to obtain the efficiencies and an algebra based on binomial detector response to efficiency correction [19, 20, 21]. The statistical uncertainty estimation is based on the numerical error propagation method of multivariate cumulants [22]. The systematic uncertainties are estimated by varying different track quality cuts, tracking efficiency and conditions for particle identification.

4. Results

The centrality dependence of efficiency corrected second-order diagonal cumulants of net proton, net kaon and net charge (top to bottom) for 0-5% most central Au + Au collisions at $\sqrt{s_{NN}} = 7.7, 11.5, 14.5, 19.6, 27, 39, 62.4$ and 200 GeV are shown as a function of $\langle N_{part} \rangle$ in Fig. 1. We find a linearly increasing trend as expected from a scaling, predicted by the central limit theorem. In a given centrality, the width of net-proton distribution decreases as a function of beam energy in the range $\sqrt{s_{NN}} = 7.7-39$ GeV and then increases at top RHIC energies [8]. This is because of baryon transport that has a strong beam energy dependence.

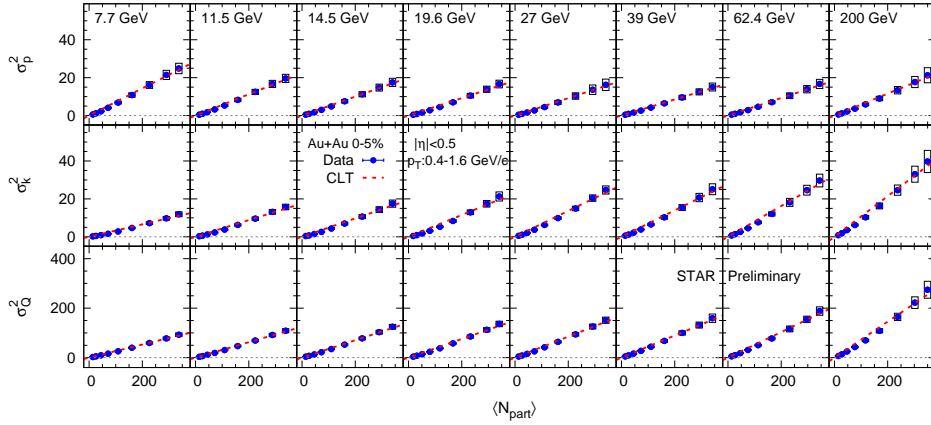


Figure 1: Centrality dependence of the second-order diagonal cumulants (variances) of net proton, net kaon and net charge (top to bottom) multiplicity distributions for Au+Au collisions at $\sqrt{s_{NN}} = 7.7-200$ GeV (left to right) within kinematic range $|\eta| < 0.5$ and $0.4 < p_T < 1.6$ GeV/c. Boxes represent systematic uncertainties. The statistical error bars are within the marker size. The red dashed lines represent a scaling predicted by central limit theorem.

Figure 2 shows the efficiency corrected second-order off-diagonal cumulants of net-charge, net-proton, net-kaon multiplicity distributions for Au+Au collisions at eight colliding energies. The off-diagonal cumulants between net-charge–net-kaon ($\sigma_{Q,k}^{1,1}$) and that of net-charge–net-proton ($\sigma_{Q,p}^{1,1}$) increase with centrality. On the contrary, there is a growing anti-correlation behaviour observed between net-proton and net-kaon ($\sigma_{p,k}^{1,1}$) with centrality at $\sqrt{s_{NN}} > 19.6$ GeV.

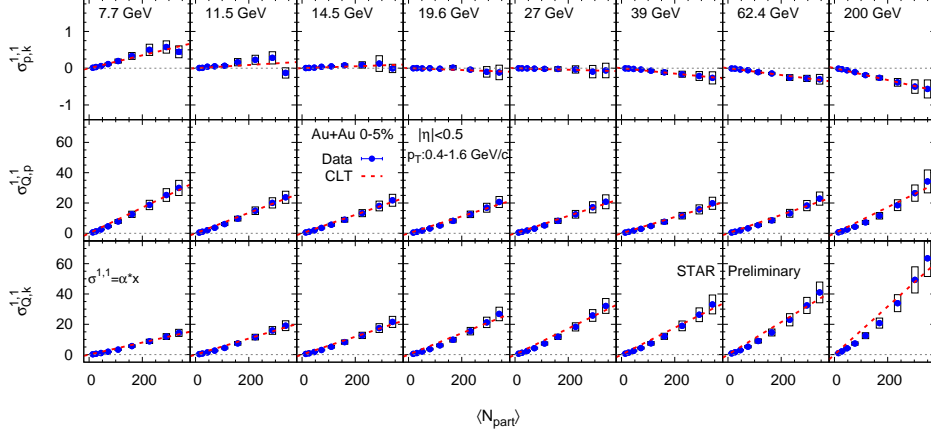


Figure 2: Centrality dependence of the second-order off-diagonal cumulants (covariances) of net-proton, net-charge and net-kaon for Au+Au collisions at $\sqrt{s_{NN}} = 7.7$ -200 GeV (left to right) within kinematic range $|\eta| < 0.5$ and $0.4 < p_T < 1.6$ GeV/c. Boxes represent systematic uncertainties. The statistical error bars are within the marker size. The red dashed lines represent a scaling predicted by central limit theorem.

Figure 3 shows the off-diagonal to diagonal cumulant ratios $C_{p,k} = \sigma_{p,k}^{1,1}/\sigma_k^2$, $C_{Q,k} = \sigma_{Q,k}^{1,1}/\sigma_k^2$ and $C_{Q,p} = \sigma_{Q,p}^{1,1}/\sigma_p^2$ (top to bottom) as a function of beam energy for most central (0-5%) and peripheral (70-80%) collisions. These cumulant ratios are designed to eliminate the effect of system volume. An excess correlation is observed in $C_{Q,p}$ and $C_{Q,k}$ in 0-5% most central in comparison to the peripheral collisions. The values of $C_{Q,p}$ and $C_{Q,k}$ are observed to increase with beam energy, and this increasing trend cannot be explained by the HRG and UrQMD model calculations. It is observed that the normalized p - k correlation ($C_{p,k}$) is positive at the lowest BES energy and negative at higher energies. For 0-5% top central bins, $C_{p,k}$ changes sign around 19.6 GeV.

5. Summary

The second-order diagonal and off-diagonal cumulants of net proton, net kaon, and net charge multiplicity distributions in Au+Au collisions from the RHIC BES-I program in the energy range of $\sqrt{s_{NN}} = 7.7$ -200 GeV are presented. Significant excess correlation is observed in $C_{Q,p}$ and $C_{Q,k}$ in central in comparison with peripheral events. Both HRG and UrQMD model underpredict the data and cannot describe the increasing with beam energy trends of $C_{Q,p}$ and $C_{Q,k}$. The value of $C_{p,k}$ in 0-5% central collision is found to be negative at $\sqrt{s_{NN}} = 200$ GeV and positive at $\sqrt{s_{NN}} = 7.7$ GeV. The measurements of the full second-order cumulant matrix elements of net- $p/k/Q$ multiplicity distributions as a function of centrality and beam energy will improve the estimation of freeze-out parameters by theoretical calculations and that help to map the QCD phase diagram. For more details of this analysis we refer the readers to Ref. [1].

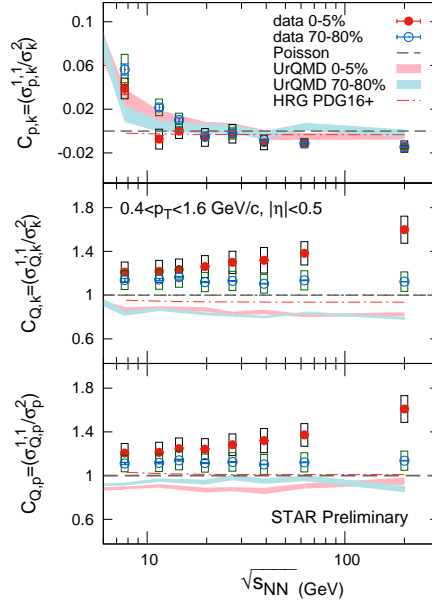


Figure 3: Beam energy dependence of cumulants ratios $C_{p,k}$, $C_{Q,k}$ and $C_{Q,p}$ (top to bottom) for Au+Au collisions at $\sqrt{s_{NN}} = 7.7-200$ GeV (left to right). The bands denote the UrQMD data for 0-5% and 70-80% central collisions and Poisson baseline is denoted by dotted lines. Error bars and boxes represent statistical and systematic uncertainties, respectively.

References

- [1] STAR collaboration, *Collision energy dependence of second-order off-diagonal and diagonal cumulants of net-charge, net-proton and net-kaon multiplicity distributions in Au+Au collisions*, 1903.05370.
- [2] M. A. Stephanov, *Non-Gaussian fluctuations near the QCD critical point*, *Phys. Rev. Lett.* **102** (2009) 032301.
- [3] S. Jeon and V. Koch, *Event by event fluctuations*, hep-ph/0304012.
- [4] X. Luo, *Exploring the QCD Phase Structure with Beam Energy Scan in Heavy-ion Collisions*, *Nucl. Phys.* **A956** (2016) 75.
- [5] STAR collaboration, *Beam energy dependence of moments of the net-charge multiplicity distributions in Au+Au collisions at RHIC*, *Phys. Rev. Lett.* **113** (2014) 092301.
- [6] PHENIX collaboration, *Measurement of higher cumulants of net-charge multiplicity distributions in Au+Au collisions at $\sqrt{s_{NN}} = 7.7 - 200$ GeV*, *Phys. Rev.* **C93** (2016) 011901.
- [7] STAR collaboration, *Higher Moments of Net-proton Multiplicity Distributions at RHIC*, *Phys. Rev. Lett.* **105** (2010) 022302.
- [8] STAR collaboration, *Energy Dependence of Moments of Net-proton Multiplicity Distributions at RHIC*, *Phys. Rev. Lett.* **112** (2014) 032302.
- [9] STAR collaboration, *Collision Energy Dependence of Moments of Net-Kaon Multiplicity Distributions at RHIC*, *Phys. Lett.* **B785** (2018) 551.

- [10] V. Koch, A. Majumder and J. Randrup, *Baryon-strangeness correlations: A Diagnostic of strongly interacting matter*, *Phys. Rev. Lett.* **95** (2005) 182301.
- [11] HOTQCD collaboration, *Fluctuations and Correlations of net baryon number, electric charge, and strangeness: A comparison of lattice QCD results with the hadron resonance gas model*, *Phys. Rev. D* **86** (2012) 034509.
- [12] F. Karsch, *Conserved charge fluctuations at vanishing and non-vanishing chemical potential*, *Nucl. Phys. A* **967** (2017) 461.
- [13] A. Majumder and B. Muller, *Baryonic strangeness and related susceptibilities in QCD*, *Phys. Rev. C* **74** (2006) 054901.
- [14] A. Chatterjee, S. Chatterjee, T. K. Nayak and N. R. Sahoo, *Diagonal and off-diagonal susceptibilities of conserved quantities in relativistic heavy-ion collisions*, *J. Phys.* **G43** (2016) 125103.
- [15] X. Luo, J. Xu, B. Mohanty and N. Xu, *Volume fluctuation and auto-correlation effects in the moment analysis of net-proton multiplicity distributions in heavy-ion collisions*, *J. Phys.* **G40** (2013) 105104.
- [16] STAR collaboration, *Systematic Measurements of Identified Particle Spectra in pp, d^+ Au and Au+Au Collisions from STAR*, *Phys. Rev. C* **79** (2009) 034909.
- [17] N. R. Sahoo, S. De and T. K. Nayak, *Baseline study for higher moments of net-charge distributions at energies available at the BNL Relativistic Heavy Ion Collider*, *Phys. Rev. C* **87** (2013) 044906.
- [18] X. Luo and N. Xu, *Search for the QCD Critical Point with Fluctuations of Conserved Quantities in Relativistic Heavy-Ion Collisions at RHIC : An Overview*, *Nucl. Sci. Tech.* **28** (2017) 112.
- [19] M. Kitazawa and M. Asakawa, *Relation between baryon number fluctuations and experimentally observed proton number fluctuations in relativistic heavy ion collisions*, *Phys. Rev. C* **86** (2012) 024904.
- [20] A. Bzdak and V. Koch, *Acceptance corrections to net baryon and net charge cumulants*, *Phys. Rev. C* **86** (2012) 044904.
- [21] X. Luo, *Unified description of efficiency correction and error estimation for moments of conserved quantities in heavy-ion collisions*, *Phys. Rev. C* **91** (2015) 034907.
- [22] “The effect of efficiency correction and error calculations are implemented in the open-source package, SMoment. The code package can be downloaded from <https://github.com/ptribedy/SMoment>.”